Cairo University

Journal of Advanced Research

ORIGINAL ARTICLE

Effect of bulk and nano-Fe_2O_3 particles on peanut plant leaves studied by Fourier transform infrared spectral studies

CrossMark

S. Suresh [a,b,*], S. Karthikeyan [a,c], K. Jayamoorthy [d]

[a] *Research and Development Center, Bharathiar University, Coimbatore 641 046, Tamil Nadu, India*
[b] *Department of Physics, St.Joseph's College of Engineering, Chennai 600 119, Tamil Nadu, India*
[c] *Department of Physics, Dr.Ambedkar Government Arts College, Chennai 600 039, Tamil Nadu, India*
[d] *Department of Chemistry, St.Joseph's College of Engineering, Chennai 600 119, Tamil Nadu, India*

A B S T R A C T

The interaction of metal oxide nanoparticles with plants has not been extensively studied. An attempt has been made to examine the potential variation in peanut plant leaves due to the application of Fe_2O_3 nanoparticle by pre-sowing technique and to compare with its bulk counterpart. Fe_2O_3 nanoparticle was synthesized by chemical route and characterized using X-ray diffraction, atomic force and scanning electron microscopy. The Fe_2O_3 nanoparticle and its bulk counterpart are applied to the peanut seeds by pre-soaking method at two different concentrations: 500 and 4000 ppm. A total of three replicates were chosen for each morphological and physiological measurement (at an average of three plants per replica). The Fourier transform infrared spectral analysis shows the most prominent peaks at 2923 and 1636 cm^{-1}, and other peaks vary due to Fe_2O_3 stress, which was confirmed by the calculated mean ratio of the peak intensities for various frequency regions. All leaf samples show considerable increase in glycoprotein, with 500 ppm bulk and 4000 ppm nano-Fe_2O_3 samples exhibiting a maximum increase of 73.86% and 71.45%, respectively. The total amide I and II protein content of leaf sample soaked in 500 ppm bulk Fe_2O_3 suspension decreased to a greater extent compared with other leaf samples. The leaf samples soaked in 500 ppm concentration of both bulk and nano-Fe_2O_3 suspension exhibited lower lipid content with total band area of 76.97 ± 0.832 and 76.31 ± 0.468, respectively. The cumulative percentage of explained

* Corresponding author. Tel.: +91 9884633846.
E-mail address: profsuresh1@gmail.com (S. Suresh).
Peer review under responsibility of Cairo University.

Production and hosting by Elsevier

variance in secondary structure of protein of all leaf samples is 83.888% in which factor 1 accounts for 51.870% and factor 2 accounts for 32.018% of the total data variance. The principal component (PC) loadings plot for the spectral range 1600–1700 cm^{-1} clearly shows that the PC1 factor might establish the maximum variation of the secondary structure of protein in leaf samples.

Introduction

Micronutrients play a vital role in plant nutrition and growth. Iron is one of the essential elements for plant growth and crucial in photosynthetic reactions, activating numerous enzymes, which are involved in the transfer of energy, reduction and fixation of nitrogen, formation of lignin, and contributing in RNA synthesis [1]. Furthermore, in plants, several reactions are catalyzed by compounds containing both iron and sulfur. Yellow leaves, which indicate low levels of chlorophyll, are a manifestation of iron deficiency. Leaf yellowing is first witnessed in the interveinal tissues of younger upper leaves, while completely yellow or almost white leaves indicate severe deficiency; later, the leaves turn brown and eventually die. Nevertheless, in the aerobic cellular medium, Fe insolubility and toxicity may constitute a major problem and all organisms have evolved strategies to preserve Fe homeostasis regardless of its extracellular concentration. The strategies include transportation by chelating to organic acids or transferrin, compartmentation in the apoplast space and vacuoles, storage in ferritin, and the avoidance of the reaction with peroxides by subcellular compartmentation and by the presence of high levels of antioxidants. According to Graham et al. [2] throughout the world more than 3 billion people suffer from micronutrient deficiencies. This led to research towards developing technologies for increased uptake and accumulation of micronutrients in comestible plant parts.

Peanuts (*Arachis hypogaea* L.) contain rich oil and protein, and are an important source of oil in processing industry. In some cases, peanut also serves as a supplementary food due to its high nutrition. They are extremely rich in vitamin B. They also stand out because of their high fat and protein contents. Peanut is cultivated in 108 countries. In India, peanut is grown in approximately 8 million hectares and is a popular legume food crop. The average productivity of peanut in India is far less at ~1178 kg ha^{-1} compared with the world's average 1400 kg ha^{-1}. The reason for low productivity is that the crop largely grown in rain-fed, low-fertile soils. Nanotechnology has the potential to revolutionize agriculture with new tools to enhance the ability of plants to absorb nutrients. Nanoparticles interact at molecular level in living cells and nano-agriculture involves the employment of nanoparticles in agriculture expecting that these particles impart some beneficial effects to the crop in seed germination, control of plant diseases and so on. Using nanoparticles and nanopowders, controlled- or delayed-release fertilizers can be developed. Nanoparticles are highly reactive owing to specific surface area, high-density reactive areas, or increased reactivity of these areas on the particle surfaces. These features facilitate easy absorption of pesticides and fertilizers produced in nanoscale [3]. Broadcast, foliar spray and pre-sowing seed treatment methods were used for the application of micronutrients. To decrease the expenditure and obtain better income, pre-sowing seed treatment of micronutrients is a good technique. A method for economizing the use of fertilizer, which involves soaking the cereal seeds in nutrient solution before sowing, has been reported [4–6]. Furthermore, they stated that adequate amounts of deficient elements could be added in this manner to assist the plant through the critical stages of early growth and to contribute in the significant increase of yield parameters.

Although iron toxicity is not common, some plants show symptoms, which include bronzing and stippling of leaves. Controlling free radicals, which are formed due to high iron levels, by the enzymes produced by the plants causes leaf discoloration. Some plants that are prone to iron toxicity include tomatoes, basil, *Phlox* and *Impatiens*. Fe_3O_4 ENPs in *Arabidopsis thaliana* did not significantly affect seed germination and the number of new leaves, whereas the root elongation was negatively influenced at all exposure concentrations (400, 2000, and 4000 mg/L of Fe_3O_4 nanoparticle suspensions) [7]. Ionic iron showed only slight toxicity effects at 1570 mg/L and, therefore, no median effect concentrations were determined. Microscopic examinations did not reveal ENPs in palisade cells or xylem. Apparently, aggregates of NZVI (nanoscale zerovalent iron) were found in *Sinapis alba* and *Sorghum saccharatum*, although false positives during sample preparation cannot be excluded [8].

Many works focused on the application of nanoparticles to improve the germination percentage but none of the works studied the potential variation in fully grown plant due to soaking seeds in nanoparticle-dispersed suspension. In this work, the effects of pre-sowing peanut seeds in nanoparticle and bulk Fe_2O_3 suspension are studied to ascertain the effect of nanoparticle on peanut plant leaves [4–6]. The entire plant can be analyzed for potential variations due to nanoparticles but leaves are the most sensitive part of a plant that could respond to any toxins showing symptoms such as leaf chlorosis and bull's eyespot. Hence, plant leaves were analyzed, as iron is involved in chlorophyll formation and its deficiency will cause an abnormal condition of the leaves – chlorosis.

Experimental

Synthesis of nanoparticles

The Fe_2O_3 nanoparticle was synthesized by chemical precipitation method. The solution of ferric nitrate, the precursor material, was taken in a beaker and stirred well using a magnetic stirrer. Ammonium hydroxide solution was added in drops

to form iron hydroxide precipitate. The solution was continuously stirred to avoid agglomeration of precipitated particles. The precipitate was washed several times with distilled water and annealed at 400 °C for 4 h to remove the water content and form Fe$_2$O$_3$ nanoparticle.

Characterization of Fe$_2$O$_3$ nanoparticle

The average grain size was determined from the XRD patterns using the Debye–Scherrer formula: $\tau = 0.9\lambda/\beta \cos\theta$, where wavelength ($\lambda$) of Cu K$\alpha_1$ is 1.54060 Å, and β is the full width half maximum of the most intense peak (1 0 4). X-ray diffraction (XRD) patterns were recorded on an X-ray powder diffractometer (Rich Seifert, Model 3000). Scanning electron microscope (JEOL JSM-6360) was used for sample analysis. The surface topology was investigated by using AFM Seiko SPI3800N (series SPA-400; Tokyo, Japan).

Seed preparation and presoaking

The peanut seeds were obtained from the Regional Agricultural Research Institute, Virudhachalam, India. The seeds were sterilized in a 1:8 (volume) solution of 5% sodium hypochloride and water for 5–10 min, and then rinsed thoroughly several times with deionized water. The seeds were then treated with two different concentrations of both bulk and nano-Fe$_2$O$_3$ suspension (500 and 4000 ppm) for 10 h. The nano and bulk Fe$_2$O$_3$ suspensions were prepared by ultrasonification of the solution for 1 h. Later, the seeds were sowed in separate pots for each concentration of both nano and bulk Fe$_2$O$_3$ metal oxides. The seeds were watered periodically and the leaves were collected after 30 days. A total of three replicates were chosen for each morphological and physiological measurement (at an average of three plants per replica).

FT-IR spectral analysis

The leaf samples were removed from the plant collected after 30 days of sowing. All the leaf samples were oven-dried at 100 °C for 48 h to remove moisture and ground to fine powder. The infrared spectra of leaves were recorded using KBr pellet technique in FT-IR spectrometer (BRUKER IFS 66V model) in the 4000–400 cm^{-1} region. For each spectrum, 100 scans were co-added at a spectral resolution of 4 cm^{-1}. The spectrometer was purged continuously with dry nitrogen. The frequencies for all sharp bands were accurate to 0.001 cm^{-1}. Each sample was scanned under the same conditions with three different pellets and these replicates were averaged. Baseline method was used to calculate the absorption intensity of the peaks. Care was taken to ensure that the pellets were of same thickness by applying same pressure to the same amount of the sample. Hence, directly relating the intensities of the absorption bands to the concentration of the corresponding functional groups is possible [9]. The spectra were analyzed using Origin 8.0 software (OriginLab Corporation, Massachusetts, USA).

For discussion, the samples were named L^1, L^2, L^3 and L^4, where

L^1 – leaf samples of plant seeds soaked in 500 ppm bulk Fe$_2$O$_3$ suspension collected after 30 days of sowing,

L^2 – leaf samples of plant seeds soaked in 4000 ppm bulk Fe$_2$O$_3$ suspension collected after 30 days of sowing,

L^3 – leaf samples of plant seeds soaked in 500 ppm nano-Fe$_2$O$_3$ suspension collected after 30 days of sowing,

L^4 – leaf samples of plant seeds soaked in 4000 ppm nano-Fe$_2$O$_3$ suspension collected after 30 days of sowing.

For many plant species, EC$_{50}$ values of iron oxide nanoparticles have been reported to be more than 5000 ppm [10]; hence, 4000 ppm was chosen as the higher concentration.

Statistical analysis

Statistical analyses were performed using SPSS 16.0 software. Principle component analysis (PCA) was carried out to determine the factors that influence the variation in secondary structure protein among the leaf samples treated with bulk and nano-Fe$_2$O$_3$ compared with control sample [11,12]. For data analysis, the region of 1700–1600 cm^{-1} of the FTIR spectra was baseline-corrected using the rubber band method with vector normalized and mean-centered. Then, the data were used for PCA, which removes the redundancy of data points varying in a correlated way by transforming the original data into a set of new and uncorrelated principal components (PCs). The two-factor loadings were plotted to collect information on the principal components responsible for variability in the fingerprint region of the IR spectrum. Graphical work was carried out using Origin software 8.0.

Results and discussion

XRD, SEM and AFM analyses of Fe$_2$O$_3$ nanoparticles

Fig. 1 visualizes the XRD pattern of Fe$_2$O$_3$ nanoparticle, which confirms the formation of Fe$_2$O$_3$ phase in 400 °C annealed sample. The average particle size of the nanoparticle was found to be 21 nm. The peaks were matched using JCPDS software and it was well matched with the Fe$_2$O$_3$ of file no
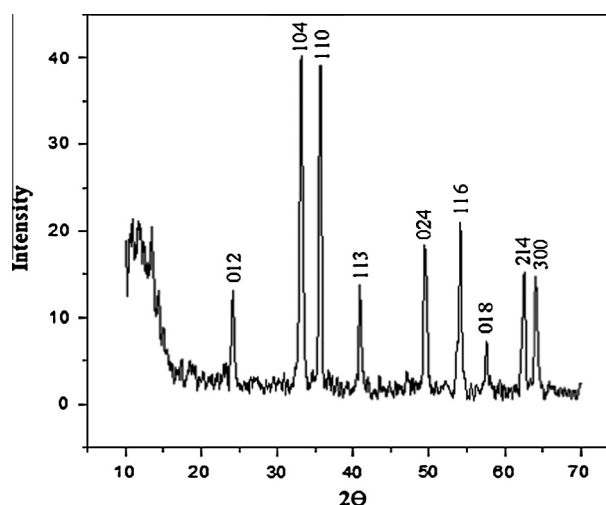

Fig. 1 XRD pattern of Fe$_2$O$_3$ nanoparticles.
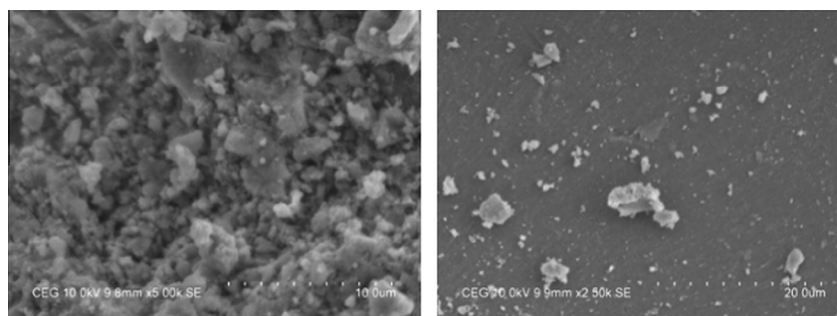
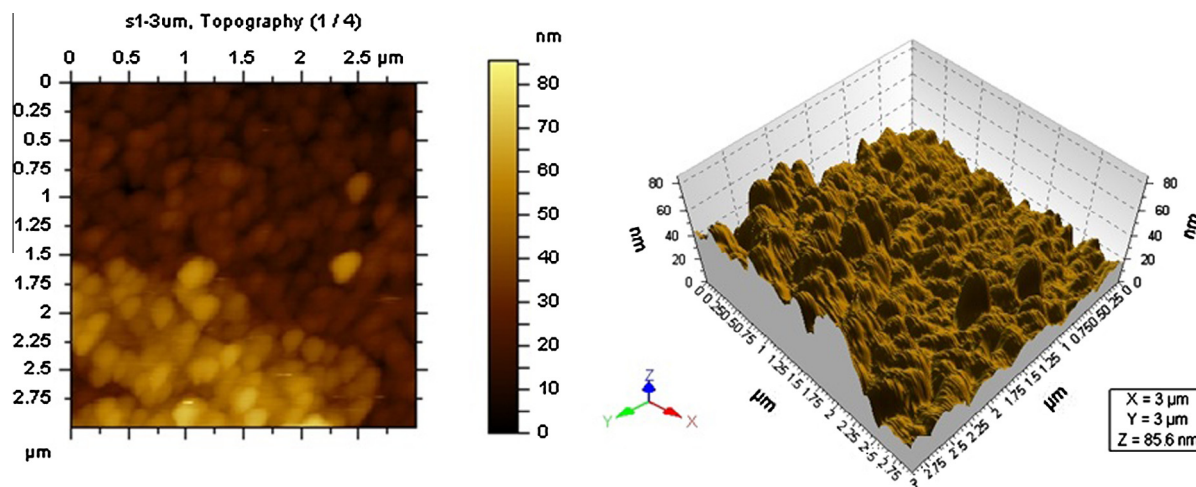**Fig. 2**   SEM images of Fe_2O_3 nanoparticles.

Fig. 3   The 2D and 3D atomic force microscopy images of Fe_2O_3 nanoparticles.

"Pdf # 892810". The SEM image confirms the uniformity of phase formation and the particle size of the Fe_2O_3 nanoparticle. Fig. 2 visualizes the SEM image of Fe_2O_3 nanoparticle.

The 2D and 3D atomic force microscopy images of iron oxide nanoparticle confirm that the particle size exists in nanorange. The average particle size of the iron oxide calculated from XRD results nearly matches with AFM results as shown in Fig. 3.

FTIR spectral studies of leaf samples

The tentative frequency assignment of averaged spectra for the peanut leaf samples collected after 30 days of sowing is shown in Table 1 and spectra are shown in Fig. 4. The strong characteristic band from $\sim$3405 cm^{-1} to $\sim$3422 cm^{-1} in all the samples is assigned to the O—H or N—H stretching of amide A. The band at $\sim$2954 cm^{-1} was absent in L^1 leaf sample but a weak band is observed in all other samples. The CH_3 symmetric stretching and CH_2 asymmetric stretching of lipid, protein band at $\sim$2923 and $\sim$2853 cm^{-1}, respectively, show elevated intensity in L^4, L^1 and L^2 leaf samples. The very strong band at $\sim$1734 cm^{-1} was absent in L^1 and L^3 leaf samples, which shows some decrease in lipids content of these samples compared with the L^2 and L^4 samples. The amide I protein is present in all the samples, which was observed from the very strong band at $\sim$1636 cm^{-1}. A very weak band at $\sim$1556 cm^{-1} indicates the presence of amide II in leaf sample

soaked in L^3 sample but it was not present in other samples indicating the influence of protein variation in these samples. The bands at $\sim$1238 cm^{-1}, $\sim$1138 cm^{-1}, and $\sim$977 cm^{-1} were present only in L^3 leaf sample, which shows that the influence of carbohydrates and other nucleic acids is slightly higher in this sample compared with other samples. The other characteristic frequencies were evenly poised in all the samples (Table 1). From these results, it can be understood that the pre-soaking with Fe_2O_3 nanoparticle suspension of 500 ppm concentration might have some positive effects such as increase in protein content and carbohydrates; however, at higher concentrations there may be some negative effects on the biological contents of these samples. Many peaks were hidden in the raw FT-IR spectra, which can be unleashed by deconvolution and derivative spectra [13]. The spectral regions between 3200 and 3450 cm^{-1}, 3000 and 2800 cm^{-1}, 1800 and 1500 cm^{-1}, and 1200 and 1000 cm^{-1} were chosen to analyze amide A and B proteins, lipids, proteins, and carbohydrates, respectively [14,15].

Table 2 shows the total band area calculated for all the Fe_2O_3 soaked samples and compared with the control leaf sample. The total band area of the 1000–2000 cm^{-1} region in all the samples shows a considerable increase, which in turn denotes the rise in carbohydrates when compared with the control sample, and the maximum variation in carbohydrate content was found in L^3 leaf sample with a band area value of 103.24 $\pm$ 0.0349. The total amide I and II protein content of

Table 1 Tentative frequency assignment of FTIR spectra for the peanut leaf samples collected after 30 days.

Control	Fe₂O₃ bulk		Fe₂O₃ nano		Tentative frequency assignment
	L^1	L^2	L^3	L^4	
3417 (vs)	3417 (vs)	3405 (vs)	3422 (vs)	3413 (vs)	Bonded O─H stretching/N─H stretching
2955 (vw)	–	2954 (vw)	2955 (vw)	2954 (vw)	CH₃ symmetric stretching; lipid, protein
2923 (m)	2921 (s)	2919 (s)	2923 (m)	2919 (s)	CH₂ asymmetric stretching; mainly lipid, protein
2853 (w)	2851 (m)	2852 (m)	2854 (w)	2851 (m)	CH₂ symmetric stretching; lipid, protein
–	–	2366 (w)	2366 (w)	–	
1734 (vw)	–	1734 (vw)	–	1734 (vw)	Carbonyl C═O stretch: lipids
1636 (vs)	1631 (vs)	1623 (vs)	1630 (vs)	1636 (vs)	Amide I: C═O stretching of proteins
–	–	–	1556 (vw)	–	Amide II: N─H Bending/C─N stretching of proteins
1425 (w)	1414 (m)	1424 (m)	1425 (w)	1424 (m)	C─N stretching/in-plane OH bending
1388 (w)	1385 (m)	1387 (w)	1376 (m)	1388 (w)	CH₃ symmetric bending; protein
1260 (vw)	1255 (vw)	1262 (vw)	1272 (m)	1260 (vw)	C-0 stretching (ethers)/C─N stretching (amines)
–	–	–	1238 (s)	–	PO2 – asymmetric stretch: mainly nucleic acids
–	–	–	1138 (m)	–	CH deformation, C─O, C─C stretching (carbohydrates)
1105 (vw)	1104 (vw)	1108 (w)	1108 (w)	–	
1098 (w)	1098 (vw)	1099 (w)	1099 (w)	1099 (w)	PO2 – symmetric stretch: mainly nucleic acids
1056 (w)	1070 (m)	1072 (w)	1055 (m)	1071 (m)	
1035 (vw)	1032 (vw)	1035 (vw)	1034 (vw)	1035 (vw)	C─O stretching/C─O bending of the C─O─H carbohydrates
–	–	–	977 (m)	–	C─N⁺─C symmetric stretch: nuclei acids
931 (vw)	934 (vw)	930 (vw)	930 (w)	930 (w)	CH out of plane bending (carbohydrate)
898 (vw)	899 (vw)	899 (vw)	898 (vw)	895 (vw)	Carbonate asymmetric stretching
–	–	857 (w)	856 (w)	855 (w)	CH out of plane bending (carbohydrate)
839 (vw)	–	833 (vw)	843 (w)	–	
–	–	–	767 (m)	–	CH₂ bending, carbohydrates, proteins and lipids (sterols of fatty acids)
663 (vw)	663 (vw)	664 (vw)	666 (w)	665 (w)	
611 (vw)	–	612 (vw)	612 (w)	612 (w)	C─O─O, P─O─C bonding (aromatics) phosphate

vs – very strong, s – strong, m – medium, w – weak, vw – very weak.
L^1 – Leaf samples of plant seeds soaked in 500 ppm Fe₂O₃ bulk suspension collected after 30 days of sowing, L^2 – leaf samples of plant seeds soaked in 4000 ppm Fe₂O₃ bulk suspension collected after 30 days of sowing, L^3 – leaf samples of plant seeds soaked in 500 ppm Fe₂O₃ nanosuspension collected after 30 days of sowing, L^4 – leaf samples of plant seeds soaked in 4000 ppm Fe₂O₃ nanosuspension collected after 30 days of sowing.
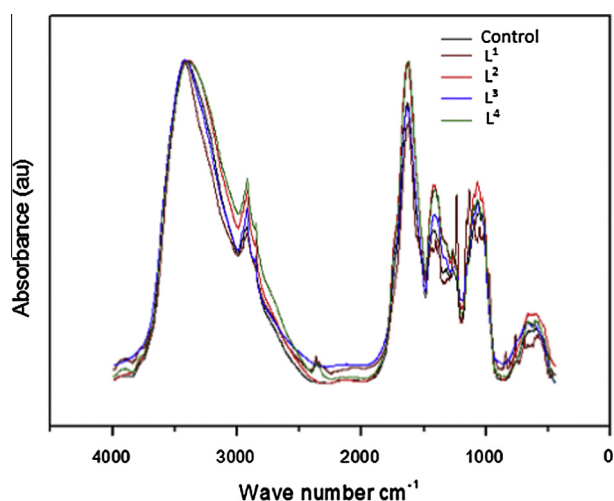

Fig. 4 FT-IR spectra for the peanut leaf samples collected after 30 days.

L^1 leaf sample is decreased to a greater extent, whereas protein contents of the L^2, L^3 and L^4 leaf samples are approximately close to the control sample, which was clearly observed from the calculated band area in the region 1500–1800 cm⁻¹. Also, the comparison between the samples denotes low band area value of 95.55 ± 0.983 in L^1 leaf sample, which shows the

greater impact on total amide I and II protein content when soaked in Fe₂O₃ bulk suspension of 500 ppm concentration. The region around 2800–3000 cm⁻¹ contributes mainly to the lipid content of the leaf samples, which was found to decrease in all the leaf samples when compared with the control leaf sample. The leaf samples soaked in 500 ppm concentration of both bulk and nano-Fe₂O₃ suspension have lower lipid content with total band area of 76.97 ± 0.832 and 76.31 ± 0.468, respectively, but total area of control leaf sample was found to be 91.69 ± 0.856. In contrast to the total amide I and II protein variation of the leaf samples, the amide A protein was very low in L^3 leaf sample alone with total band area of 74.48 ± 0.623, and all other leaf samples increase when compared with control leaf sample of band area 101.10 ± 0.152.

The mean ratio of the peak intensities of the bands at 1547 cm⁻¹ and at 3296 cm⁻¹ (I_{1547}/I_{3296}) was used as an indicator of the relative concentration of the amide II and amide A protein in the leaf samples (Table 3). In the present work, the calculated ratio of L^1, L^2 and L^4 corresponds to 37.99%, 12.24% and 17.69% decrease in protein compared with the control. On the contrary, the protein content increases by 18.66% in L^3 sample alone. The mean ratio of the intensity of absorption of the methyl and methylene bands (I_{2951}/I_{2858}) decrease by 17.06%, 18.85%, and 17.19% in L^1, L^2 and L^4, respectively. The decrease in the ratio indicate a decrease in the number of methyl groups in protein fibers compared with methylene groups in these leaf samples. However, there is no

Table 2 The total band area calculated for all the leaf samples pre-soaked with Fe_2O_3 suspension and compared with the control leaf sample.

Total band area	Control	L[1]	L[2]	L[3]	L[4]
1000–1200	78.46 ± 0.2	95.90 ± 0.05 (+22.23)	92.18 ± 0.1 (+17.49)	103.24 ± 0.03 (+31.58)	85.71 ± 0.3 (+9.24)
1500–1800	113.27 ± 1.2	95.55 ± 0.9 (−15.64)	108.73 ± 1.5 (−4.01)	110.09 ± 0.5 (−2.81)	110.13 ± 0.5 (−2.77)
2800–3000	91.69 ± 0.8	76.97 ± 0.8 (−16.05)	84.94 ± 0.2 (−7.36)	76.31 ± 0.4 (−16.77)	90.71 ± 1.02 (−1.07)
3200–3450	101.10 ± 0.1	107.02 ± 0.2 (+5.86)	107.51 ± 0.4 (+6.34)	74.48 ± 0.6 (−26.33)	102.09 ± 0.4 (+0.98)

Values in parentheses represent percent increase (+) or decrease (−) over control values.
The values are the mean ± S.E. for each group. The number of replicates is 3.
L[1] – Leaf samples of plant seeds soaked in 500 ppm Fe_2O_3 bulk suspension collected after 30 days of sowing, L[2] – leaf samples of plant seeds soaked in 4000 ppm Fe_2O_3 bulk suspension collected after 30 days of sowing, L[3] – leaf samples of plant seeds soaked in 500 ppm Fe_2O_3 nanosuspension collected after 30 days of sowing, L[4] – leaf samples of plant seeds soaked in 4000 ppm Fe_2O_3 nanosuspension collected after 30 days of sowing.

Table 3 Mean ratio of peak intensities of the bands at different wave numbers.

Ratio of bands	Control	L[1]	L[2]	L[3]	L[4]
1547/3296	0.9918 ± 0.012	0.6150 ± 0.006 (−37.99)	0.8704 ± 0.003 (−12.24)	1.1769 ± 0.015 (+18.66)	0.8164 ± 0.006 (−17.69)
2951/2858	1.1021 ± 0.022	0.9141 ± 0.019 (−17.06)	0.8943 ± 0.001 (−18.85)	1.1011 ± 0.008 (−0.091)	0.9127 ± 0.011 (−17.19)
1547/1656	0.6265 ± 0.001	0.6002 ± 0.013 (−4.20)	0.5868 ± 0.001 (−6.34)	0.5769 ± 0.002 (−7.92)	0.7095 ± 0.003 (13.25)
1083/1547	1.1417 ± 0.025	1.9850 ± 0.003 (+73.86)	1.4279 ± 0.023 (+25.07)	1.4242 ± 0.012 (+24.74)	1.9575 ± 0.010 (+71.45)
1743/1458	0.9071 ± 0.009	0.5196 ± 0.006 (−42.72)	1.1154 ± 0.021 (+22.96)	0.8964 ± 0.001 (−1.18)	0.7392 ± 0.005 (−18.51)
1743/1547	1.1714 ± 0.003	0.9850 ± 0.011 (−15.91)	1.3692 ± 0.009 (+16.89)	1.0747 ± 0.004 (−8.26)	1.1630 ± 0.022 (−0.72)
1458/1547	1.2914 ± 0.017	1.8957 ± 0.014 (+46.79)	1.2276 ± 0.007 (−4.94)	1.1989 ± 0.011 (−7.16)	1.5734 ± 0.014 (+21.84)

Values in parentheses represent percent increase (+) or decrease (−) over control values.
L[1] – Leaf samples of plant seeds soaked in 500 ppm Fe_2O_3 bulk suspension collected after 30 days of sowing, L[2] – leaf samples of plant seeds soaked in 4000 ppm Fe_2O_3 bulk suspension collected after 30 days of sowing, L[3] – leaf samples of plant seeds soaked in 500 ppm Fe_2O_3 nanosuspension collected after 30 days of sowing, L[4] – leaf samples of plant seeds soaked in 4000 ppm Fe_2O_3 nanosuspension collected after 30 days of sowing.

considerable change in the mean intensity ratio for L[3] sample, which indicated that there is no variation in number of methyl and methylene group of proteins over control sample [16–18].

The mean ratio of the intensities of the bands at 1547 cm^{-1} and 1656 cm^{-1} (I_{1547}/I_{1656}) could be attributed to a change in the composition of the whole protein pattern [19]. The calculated mean ratio of intensities of L[1], L[2] and L[3] samples decreases in whole protein of 4.20%, 6.34%, and 7.92% in these samples, respectively. The L[4] sample of leaves shows 13.25% increase in total protein, which indicates that the seeds soaked in 4000 ppm of Fe_2O_3 nanoparticle suspension increase the total protein content, which is more unusual trend observed since the seeds soaked in 500 ppm of Fe_2O_3 nanoparticle suspension decrease the total protein such that the percent difference between these concentrations is 22.98%.

The mean ratio of peak intensities of the bands 1083 cm^{-1} and 1547 cm^{-1} (I_{1083}/I_{1547}) explains the variation in glycoprotein of the samples. All leaf samples show considerable increase in glycoprotein where L[1] and L[4] samples exhibit maximum increase of 73.86% and 71.45%, respectively. The lipid variation was analyzed from the calculated mean ratio of peak intensities of the bands 1743 cm^{-1} and 1458 cm^{-1} (I_{1743}/I_{1458}), and the results show 42.72%, 18.51% and 1.18% decrease in L[1], L[4] and L[3] leaf samples, respectively, and a 22.96% increase in L[2] leaf sample compared with the control sample. The increase in ratio suggested that lipids are being oxidized in L[2] sample. Since oxidation can cause an increase in carbonyls and a degradation of lipids, both of these changes could contribute to the elevated ratio. Furthermore, the ratio of integrated areas of both I_{1458}/I_{1547} and I_{1743}/I_{1547} is less compared with the control tissues, suggesting that lipid degradation predominates carbonyl formation.

FT-IR spectroscopy is one of the principal techniques used to determine the secondary structure of proteins. The Fourier self-deconvolution and second derivative spectra could explain in more detail about the impact of bulk and nano-Fe_2O_3 suspension on peanut plant leaves. Further analysis has been carried out by resolving the amide I band using the curve fitting method to study the secondary structure of proteins. To find out the number of peaks in the amide I region for curve-fitting process, the second derivative spectra were calculated by using Origin 8.0 software (Savitzky–Golay as a

derivative operation) in the amide I region. Derivatives gave the number and positions, as well as an estimation of the band-width and intensity of the bands making up the amide I region. After baseline correction, the best fit for decomposing the amide I bands in the spectral region of interest was obtained by Gaussian components using the same software. The underlying bands of amide I band as deduced by curve-fitting analysis for the control, and samples treated with various concentration of bulk and nano-Fe_2O_3 were tabulated. The band around 1656 cm^{-1} is assigned for α-helix of secondary structure of protein and its integrated band area is found to decrease in all the samples except in L^2 sample, which increased by 9.07%. The decrease in band area of L^3 and L^4 samples is found to be 6.38% and 9.35%, respectively, which is comparatively lesser than L^1 sample value of 29.17% variation from control sample. The band at 1633 cm^{-1} is due to the β-sheet of secondary protein structure, which shows a steep increase in the band area of 147.28%, 112.99%, 64.13% and 99.75% in L^1, L^2, L^3 and L^4 samples, respectively. The random coil of the secondary structure of protein observed from the peak centered at 1648 cm^{-1} shows decrease in the band area of all the samples considerably expect L^1 sample where a steep 66.20% increase was observed. The bands centered around 1666, 1673 and 1684 cm^{-1} were assigned for the β-turn of the secondary protein structure (Table 4). The integrated band area for 1666 cm^{-1} is found to increase in L^2, L^3 and L^4 samples by 71.78%, 152.30% and 39.93% respectively, whereas it was slightly decreased in L^1 sample by 1.62%. The integrated band area of 1673 and 1684 cm^{-1} was increased and decreased, respectively, for all the leaf samples. The percentage increase in the band area of β-sheet and β-turn and decrease in the band area of α-helix of secondary structure of protein might be due to the interaction of peanut seeds with Fe_2O_3 particles.

Principal component analysis

Furthermore, PCA using SPSS 16.0 software is performed for understanding the protein secondary structure variation among the samples treated with bulk and nano-Fe_2O_3 particles and also the variation among the frequency bands. The result in Table 5 shows that the variation of secondary structure of protein due to the Fe_2O_3 metal oxide treatment is calculated using varimax rotated factor analysis of PC extraction method.

Using rotated factor loading and commonalities varimax rotation analysis, information about the principal factors in

Table 5 Variation of secondary structure of protein due to the metal treatment is calculated using varimax rotated factor analysis of principal component extraction method.

Component	Rotation sums of squared loadings		
	Eigen value	% of Variance	Cumulative%
1	0.593	51.870	51.870
2	1.601	32.018	83.888
Sample	Component		
	1		2
L1	−0.078		0.933
L2	0.885		0.101
L3	0.903		0.099
L4	0.355		0.837
Control	0.930		0.099

L^1 – Leaf samples of plant seeds soaked in 500 ppm Fe_2O_3 bulk suspension collected after 30 days of sowing, L^2 – leaf samples of plant seeds soaked in 4000 ppm Fe_2O_3 bulk suspension collected after 30 days of sowing, L^3 – leaf samples of plant seeds soaked in 500 ppm Fe_2O_3 nanosuspension collected after 30 days of sowing, L^4 – leaf samples of plant seeds soaked in 4000 ppm Fe_2O_3 nanosuspension collected after 30 days of sowing.
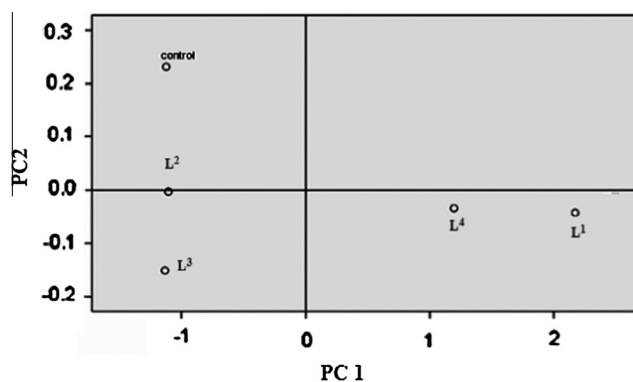

Fig. 5 Principle component analysis explained variance in secondary structure of protein of all leaf samples.

the studied samples was obtained. The successive factors account for the decreasing amounts of residual variance using two factors (varimax rotation) for the samples: control, L^1, L^2,

Table 4 Frequency assignment for secondary protein obtained by self-deconvoluted spectra in the spectral region 1600–1700 cm^{-1}.

Frequency (cm^{-1})	Assignment	Control	L^1	L^2	L^3	L^4
1633	β-sheet	1.578	3.902 (+147.28)	3.361 (+112.99)	2.590 (+64.13)	3.152 (+99.75)
1648	Random coil	4.009	2.268 (−43.43)	3.485 (−13.07)	6.663 (+66.20)	0.754 (−81.19)
1656	α-helix	5.345	3.786 (−29.17)	5.830 (+9.07)	5.004 (−6.38)	4.845 (−9.35)
1666	β-turn	3.218	3.166 (−1.62)	5.528 (+71.78)	8.119 (+152.30)	4.503 (+39.93)
1673	β-turn	2.070	5.461 (+163.82)	3.765 (+81.88)	3.658 (+76.71)	2.541 (+22.75)
1684	β-turn	6.064	2.515 (−58.53)	1.746 (−71.21)	3.375 (−44.34)	3.797 (−37.38)

Values in parentheses represent percent increase (+) or decrease (−) over control values.
L^1 – Leaf samples of plant seeds soaked in 500 ppm Fe_2O_3 bulk suspension collected after 30 days of sowing, L^2 – leaf samples of plant seeds soaked in 4000 ppm Fe_2O_3 bulk suspension collected after 30 days of sowing, L^3 – leaf samples of plant seeds soaked in 500 ppm Fe_2O_3 nanosuspension collected after 30 days of sowing, L^4 – leaf samples of plant seeds soaked in 4000 ppm Fe_2O_3 nanosuspension collected after 30 days of sowing.
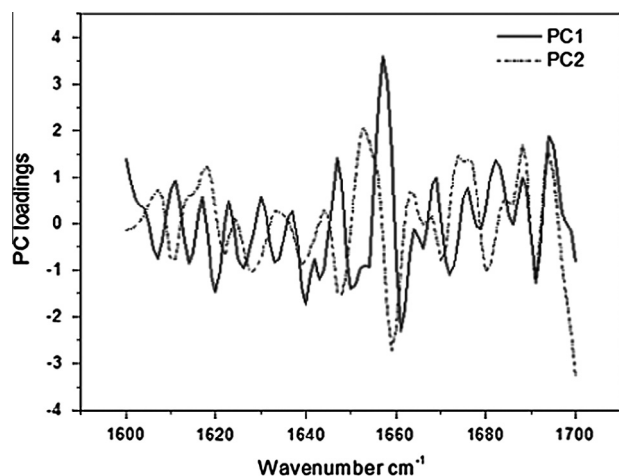
Fig. 6 PC loadings plot for the spectral range 1600–1700 cm^{-1}.

L^3 and L^4 of leaf samples. The main factor (> 0.6) for control, L^2 and L^3 is noted as factor 1, while factor 2 contributes L^1 and L^4. Factor analysis or named PCA is a useful tool in the examination of multivariate data (Fig. 5). The cumulative percentage of explained variance in secondary structure of protein of all leaf samples is 83.888%. Factor 1 accounts for 51.870% of the total data variance so the variation of secondary structure of protein was established by accounting the control, L^2 and L^3 samples. Factor 2 accounts for 32.018% which includes L^1 and L^4 samples. Fig. 6 shows the PC loadings plot for the spectral range 1600–1700 cm^{-1}, which clearly shows that the PC1 factor might establish the maximum variation of the secondary structure of protein in leaf samples compared with other components.

Conclusions

The effect of pre-soaking peanut seeds in bulk and nano-Fe_2O_3 suspension is studied extensively. The synthesized Fe_2O_3 nanoparticle was phase confirmed with XRD results and the average particle size was 21 nm. The SEM and AFM images confirm the uniformity of nanophase throughout the sample. The FT-IR results of peanut plant leaves collected after 30 days of growth period suggest that the Fe_2O_3 nanoparticle has considerable effect when applied through presoaking technique. The carbohydrate and nucleic acids of amide A and B protein of all samples have considerably increased, whereas amide I and II protein of all samples was decreased slightly, which was observed from the decrease in the calculated band area. The secondary structure of protein varies to a greater extent and the calculated results suggest that the β-sheet and β-turn of secondary structure of protein increased in all samples compared with control. The leaf samples of peanut soaked in Fe_2O_3 nanoparticle suspension with 500 ppm and 4000 ppm concentration indicate the possible greater influence over the secondary structure of protein compared with its bulk counterpart. The PCA further suggests that the control, L^2 and L^3 samples explain the total variance of the secondary structure of protein content in leaf samples of peanut plant. These results suggest that there is considerable effect on peanut plant

leaves grown by the application of nano and bulk Fe_2O_3 suspension to seeds by pre-sowing, but at lower concentration, the application of nanoparticle might have few positive effects compared with that of higher concentration.

Conflict of interest

The authors have declared no conflict of interest.

Compliance with Ethics Requirements

This article does not contain any studies with human or animal subjects.

References

[1] Malakouti M, Tehrani M. Micronutrient role in increasing yield and improving the quality of agricultural products. 1st ed. Tehran: Tarbiat Modarres Press; 2005.

[2] Graham RD, Welch RM, Bouis HE. Addressing micronutrient malnutrition through enhancing the nutritional quality of staple foods: principles, perspectives and knowledge gaps. Adv Agron 2001;70:77–142.

[3] Anonymous. Report from the mid-year fisheries assessment plenary. Stock assessments and yield estimates. Wellington (New Zealand): Ministry of Fisheries; 2009.

[4] Sathish S, Sundareswaran S, Senthil N, Ganesan KN. Biochemical changes due to seed priming in maize hybrid COH(M)5. Res J Seed Sci 2012;5(3):71–83.

[5] Maroufi K, Farahani HA, Aghdam AM. Effect of nanopriming on germination in sunflower (*Helianthus Annus* L.). Adv Environ Biol 2011;5(13):3747–50.

[6] Sharma A, Deshpande VK. Effect of pre-soaking of pigeon pea seeds with organics on seed quality. Karnataka J Agric Sci 2006;19(2):396–9.

[7] Lee CW, Mahendra S, Zodrow K, Li D, Tsai YC, Braam J, et al. Developmental phytotoxicity of metal oxide nanoparticles to Arabidopsis thaliana. Environ Toxicol Chem 2010;29:669–75.

[8] Libralato G, Devoti A Costa, Zanella Michela, Sabbioni E, Mičetić I, Manodori L, et al. Phytotoxicity of ionic, micro- and nano-sized iron in three plant species. Ecotoxicol Environ Saf. < http://dx.doi.org/10.1016/j.ecoenv.2015.07.024 02015 >.

[9] Cakmak G, Togan I, Severcan F. 17b-Estradiol induced compositional, structural and functional changes in rainbow trout liver, revealed by FT-IR spectroscopy: a comparative study with nonylphenol. Aquatic Toxicol 2006;77:53–63.

[10] Wu SG, Huang L, Head J, Chen DR, Kong IC, Tang YJ. Phytotoxicity of metal oxide nanoparticles is related to both dissolved metals ions and adsorption of particles on seed surfaces. J Pet Environ Biotechnol 2012;3:4.

[11] Surewicz WK, Mantsch HH, Chapman D. Determination of protein secondary structure by Fourier transform infrared spectroscopy: a critical assessment. Biochemistry 1993;32(2):389–93.

[12] Mecozzi M, Pietroletti M, Mento RD. Application of FTIR spectroscopy in ecotoxicological studies supported by multivariate analysis and 2D correlation spectroscopy. Vib Spectrosc 2007;44:228–35.

[13] Cakmak G, Togan I, Uduz C, Severcan F. FT-IR spectroscopic analysis of rainbow trout liver exposed to nonylphenol. Appl Spectrosc 2003;57:835–41.

[14] Lin SY, Wei YS, Hsieh TF, Li MJ. Pressure dependence of human fibrinogen correlated to the conformational α-helix to

β-sheet transition: an Fourier transform infrared study microspectroscopic study. Biopoly 2004;75:393–402.

[15] Karimm S, Bandekar J. Vibrational spectroscopy and conformation of peptides, polypeptides, and proteins. Adv Protein Chem 1986;38:181–364.

[16] Palaniappan PLRM, Nishanth T, Renju VB. Bioconcentration of zinc and its effect on the biochemical constituents of the gill tissues of Labeorohita: an FT-IR study. Infrared Phys Technol 2010;53:103–11.

[17] Carton I, Böcke U, Ofstad R, Sorheim O, Kohler A. Monitoring secondary structural changes in salted and smoked salmon muscle myofiber proteins by FT-IR microspectroscopy. J Agric Food Chem 2009;57(9):3563–70.

[18] Wei ZL, Dong L, Tian ZH. Fourier transform infrared spectrometry study on early stage of cadmium stress in clover leaves. Pak J Bot 2009;41(4):1743–50.

[19] Benedetti E, Bramanti E, Papineschi F, Rossi I, Benedetti E. Appl Spectrosc 1997;51:792–7.